Advances in coastal altimetry using SARAL/AltiKa data in a multi-platform approach

Charles Troupin[a,*], Ananda Pascual[a], Guillaume Valladeau[b], Arancha Lana[a], Emma Heslop[a], Simón Ruiz[a], Marc Torner[d], Nicolas Picot[c], Joaquín Tintoré[a,d]

[a] *Mediterranean Institute for Advanced Studies (IMEDEA), Esporles, SPAIN*
[b] *Collecte Localisation Satellites (CLS), Space Oceanography Division, Ramonville Saint-Agne, FRANCE*
[c] *Toulouse Space Centre (CST), Centre National d'Etudes Spatiales (CNES), Toulouse, FRANCE*
[d] *Balearic Islands Coastal Observing and Forecasting System (SOCIB), Palma de Mallorca, SPAIN*

Abstract

In this paper we illustrate the capability of satellite altimetry in the coastal ocean, a key technological priority for the present decade. To this end, we present the results of the G-AltiKa mission conducted along a SARAL-AltiKa track south-west of Ibiza (Balearic Islands, Western Mediterranean Sea) from 1 to 5 August 2013. The main feature of the mission is that the glider measurements are almost synchronous with the altimeter pass. The HF radar system operated by the Balearic Islands Coastal Observing and Forecasting System (SOCIB) constitutes a complementary tool to describe the circulation in the study area. The work is focused on the data processing step (interpolation, filtering, corrections) applied to the measurements and on the comparison of the geostrophic velocity across the satellite track.

The absolute dynamic topography, computed by adding filtered 1 Hz and 40 Hz along-track sea-level anomalies Mediterranean Sea Mean Dynamic Topography, and the dynamic height, computed from glider temperature and salinity, both exhibited a signal characterized by weak gradients and amplitudes (2 cm), close to the expected accuracy of the AltiKa instrument. The corresponding geostrophic velocities and the HF radar velocities projected on the SARAL/AltiKa track all depicted a north-westward coastal current with a maximal velocity larger than 20 cms^{-1}.

The lack of synopticity due to the time interval between the satellite pass

(August 1, 2013, 18:26:12 UTC) and the end of the glider transect (August 5, 2013, 04:17:22 UTC) resulted in a spatial shift between the glider and the altimeter along-track signal, around 5 km. The time evolution of the HF radar currents during the mission duration confirmed the plausibility of such a shift.

After the application of a 5 km lag to the glider dynamic height, the correlation and RMS difference between the different platforms were computed. The agreement between the altimetry, glider and HF radar cross-track velocities was synthesized in a Taylor diagram that evidenced the lowest root mean square difference (9.72 cm s^{-1}) and the highest correlation (0.64) between the velocities obtained from the glider dynamic height and those from the filtered 40 Hz sea-level anomalies. The 40 Hz data are particularly valuable as they enable us to use the SARAL-AltiKa data closer to the coast than typically possible with altimetry.

Keywords: Radar Altimetry, Meso-scale eddies, Ocean Gliders, North-western Mediterranean Sea, Ibiza Channel, HF radar, Mediterranean oceanic currents, PEACHI
PACS: 92.10.ak, 92.10.Fj

1. Introduction

Over the last two decades, the progresses in satellite altimetry and the establishment of a global network of profiling ARGO floats have constituted revolutions in physical oceanography (Le Traon, 2013), enabling the description of mesoscale processes in the open ocean. One of the main challenges of the present decade will be the study of mesoscale processes in the coastal ocean. Such a challenge can be addressed thanks to other revolutions: the

*Corresponding author
Email addresses: ctroupin@imedea.uib-csic.es (Charles Troupin), ananda.pascual@imedea.uib-csic.es (Ananda Pascual), guillaume.valladeau@cls.fr (Guillaume Valladeau), alana@imedea.uib-csic.es (Arancha Lana), eheslop@imedea.uib-csic.es (Emma Heslop), simon.ruiz@imedea.uib-csic.es (Simón Ruiz), mtorner@socib.es (Marc Torner), Nicolas.Picot@cnes.fr (Nicolas Picot), jtintore@socib.es (Joaquín Tintoré)
[1]Tel. +34 971 611835
[2]Fax. +34 971 611761

recent improvements in coastal altimetry (Cipollini et al., 2010; Vignudelli et al., 2011), the intensive use of ocean gliders (Testor et al., 2010; Ruiz et al., 2012) and the development of high-frequency radar systems (Harlan et al., 2010) .

The present work presents a cross-platform mission, G-AltiKa, performed south-west of Ibiza island (Balearic Sea, Fig. 1) in August 2013, with the objectives of processing, validating and inter-calibrating multi-platform measurements in the coastal ocean. G-AltiKa consists of a glider mission carried out along an AltiKa track, a new altimeter launched on board SARAL (SAtellite for ARgos and ALtiKa) in February 2013, and designed to measure the ocean surface topography with an unprecedented accuracy (Verron, 2013). The mission constitutes an opportunity to blend AltiKa altimetry data with multi-platform observation systems in order to examine small-scale dynamics in the Ibiza Channel. It also benefits from a new observing component, not present in the previous missions: the coastal high-frequency (HF) radar operated by the Balearic Islands Coastal Observing and Forecasting System (SOCIB, Tintoré et al., 2013).

This region is specially challenging because of the small values of the Internal Rossby Radius, on the order of 10 km, sometimes with values lower than 5 km (e.g., Gascard, 1991; Send et al., 1999; Bouché, 2003; Escudier et al., 2013), due to the strong stratification and of the processes covering a wide range of temporal and spatial scales interact. These interactions lead to intense sub-basin scale dynamics, such as mesoscale eddies (Tintoré et al., 1990; Pinot et al., 1994, 2002; Rubio et al., 2009; Amores et al., 2013) or filaments (Wang et al., 1988; La Violette et al., 1990; Salusti, 1998; Bignami et al., 2008).

Two channels play a role in the meridional exchange of properties (heat and salt) between the Balearic and the Algerian basins (García-Lafuente et al., 1995; Monserrat et al., 2008): the Ibiza Channel (80 km wide and 800 m maximal depth), which separates the Iberian Peninsula and Ibiza, and the Mallorca Channel, which separates Ibiza and Mallorca islands. The warm, fresh Atlantic Water inflows occur mainly through the Ibiza Channel. The inflows are sometimes blocked by the presence of Western Intermediate Water (WIW, Pinot et al., 2002; Mason and Pascual, 2013), resulting in a north-east diversion of the Northern Current and a junction with the Balearic Current, also described by the numerical model of Juza et al. (2013). Glider monitoring in the Ibiza Channel (Heslop et al., 2012) revealed high-frequency variability with changes of transport on the order of 1 Sv in less than one

week.

Multi-sensor approaches constitute an efficient way to study and understand the small-scale processes and vertical exchanges (e.g., Pascual et al., 2010, 2013). Recently, several missions associated ship and glider measurements with altimeter data to enhance the description of small-scale dynamics in the Western Mediterranean Sea. Ruiz et al. (2009b) combined Jason-2 altimeter data with a glider section coincident with the satellite track to describe the subduction of a chlorophyll tongue in the Alboran Sea and diagnose the strong vertical velocity at the origin of the tongue. A similar technique was applied in Ruiz et al. (2009a), as they performed glider and ship measurements under ENVISAT altimeter track in order to provide a mesoscale description of the Balearic Front. Bouffard et al. (2010) further developed the combined approach by improving the processing/editing of satellite along-track measurements, thus reaching a better compatibility between glider and altimetry measurements, while Bouffard et al. (2012) employed numerical model as an additional source of information for the multi-sensor comparison.

The present paper is focused on G-AltiKa mission description and the inter-comparison and and inter-calibration of the various platforms. Section 2 presents the various measurement platforms, with a particular attention to the processing/filtering steps. The resulting currents are compared in Section 3.

2. Data and methods

The G-AltiKa mission associated in situ data (glider) with remote-sensed measurements (satellite and radar). After a description of the different platforms (Sec. 2.1-2.3), the various steps of data processing are presented (Sec. 2.4).

2.1. Altimetric data

Altimetric data allow the computation of currents using the geostrophic balance, by combining along-track measurements of sea-level anomalies (SLA) with the Mean dynamic topography (MDT), which represents the permanent stationary component of the ocean dynamic topography.

2.1.1. Along-track sea-level anomalies

SLA data are obtained by AltiKa altimeter on board SARAL satellite. To ensure a long-term continuity of altimetry observations, SARAL ground track is expected to be/almost the same as ENVISAT mission (European Space Agency), with an exact 35-day repeat cycle. AltiKa operates at a frequency in the Ka-band (35.75 GHz), leading to improved horizontal and spatial resolutions due to the reduced altimeter footprint and the enhanced bandwidth (500 MHz), respectively, but also to a higher sensitivity to rainy and cloudy conditions (Taveneau et al., 2011; Bronner, 2013).

The track no. 16 (Fig. 1) crossed part of Ibiza island on August 1, 2013, 18:26:12 UTC. The standard 1-Hz SLA (one value every 7 km on average) measured by SARAL/Altika were produced by Ssalto/Duacs and distributed by AVISO. The 40-Hz (one value every 174 m on average) measurements were obtained from AVISO after being processed using the Prototype for Expertise on AltiKa for Coastal Hydrology and Ice (PEACHI). In particular, the reliability of AltiKa measurements for coastal hydrology is of main interest in the frame of this project, which is a CNES (Centre National dEtudes Spatiales) initiative to provide end-users reliable Ka altimeter measurements over coastal areas and in open ocean but also in continental and sea ice domains. Thus, the PEACHI prototype developed aims at improving the reliability and the accuracy of the geophysical parameters and therefore Ka altimeter measurements thanks to new or improved algorithms.

2.1.2. Mean dynamic topography

The mean dynamic topography (MDT) represents the long-term-averaged circulation. The sum of the MDT and the SLA produces the absolute dynamic topography (ADT), from which the absolute geostrophic velocity is derived using the geostrophic equations. For the Mediterranean Sea, the MDT recently developed by Rio et al. (2014) (SMDT-MED-2014) is used. The SMDT-MED-2014 was constructed with the same method as in Rio et al. (2007), but with updated datasets of drifter velocities and hydrological profiles. The spatial resolution is 0.0625° by 0.0625° (versus 0.125° by 0.125° for the previous version).

2.2. Glider

A deep Slocum glider was deployed on August 2, 2013, 09:20:57 UTC, at 38.190°N, 0.995°E, south-west of Ibiza island , approximatively on the

AltiKa track no. 16. The transect ended on August 5, 2013, 01:38:51 UTC, at 38.778°N, 1.160°E after a 74 km course.

The glider was equipped with a CTD (SeaBird Pumped CTD), a fluorometer (WetLabs FLNTU) and an oxygen sensor (Aanderaa Oxygen Optode 4330F). A total of 253 profiles (126 downcast and 127 upcast) were acquired. The depth-averaged velocity (DAV) can be estimated using the glider positioning system (GPS) as follows: the glider makes a calculation of the current experienced since its last surfacing from the difference between both estimated (dead reckoned position from heading and velocity) and its current actual location from GPS. The DAV depends on the accuracy of the on-board compass, to which a mission specific error calibration (Merckelbach et al., 2008) was applied.

The horizontal resolution (distance between two consecutive surfacings) is related to the local depth, which varied from 975 m to 90 m, at the location closest to the coast (less than 7 km, Es Vedrà island, Ibiza). In the deepest areas, the resolution was on the order of 5 km, while approaching the coast, it decreased to less than 1 km.

2.3. HF radar

The SeaSonde HF radar system by Coastal ocean dynamics applications radar (CODAR), is formed by two antennas managed by the SOCIB (Tintoré et al., 2013) and located on Ibiza and Formentera islands to monitor the transports in the easternmost part of the Ibiza Channel (Fig. 1). The radar operates at a frequency of 13.5 MHz with a 90-kHz bandwidth and provides surface currents on a 3 km-resolution grid at hourly intervals, with a range up to 74 km (400 nautical miles) offshore. The southernmost latitude covered by the radar system is 38.050°N, so that 63% of the glider trajectory was inside the radar range.

2.4. Data processing

2.4.1. Computation of dynamic height

The dynamic height (DH) is obtained by integrating the density, calculated from the glider temperature and salinity, between a level of reference to the surface. Tests with reference levels between 300 and 900 m evidenced a weak sensitivity of DH gradients to this parameter. Similar conclusions were drawn by Ruiz et al. (2009a) with glider measurements north of Mallorca. This is consistent with the background of the region where dynamics are dominated by the upper ocean (0-300 m) slope currents.

2.4.2. Spatial interpolation

With the objective of performing the platform comparisons on a common track, the MDT, 1-Hz SLA, glider DH and HF radar velocities were re-sampled onto the measurement locations of the 40 Hz satellite track, using linear interpolation. The goal is to obtain the data on a unique set of locations, so the simplest interpolation method was preferred. No extrapolation was performed because of the risk to artificially generate large gradients of SLA (and thus large velocities). The ADT is obtained by adding the interpolated MDT and SLA.

2.4.3. Filtering

In order to get rid of inertial motions and high-frequency processes not compatible with the hypothesis of geostrophy, a windowed sinc filter (e.g., Smith, 2002) with a 30-hour cut-off and a Blackman window (Blackman and Tukey, 1959) was applied to the HF radar data. A similar filter, but with a 14-km cut-off, was applied on the altimeter and glider data. This value is in line with the cut-off used in similar studies (e.g. Bouffard et al., 2010, 2012). A weak sensitivity to the cut-off length was observed. This type of filter was selected because of its good stop-band attenuation and low pass-band ripple. Other filter windows were tested but the resulting signals did not exhibit significant results. The filters were designed using the Scipy (Jones et al., 2001) Signal Processing Module.

2.4.4. Geostrophic velocity computation

The component of the geostrophic current perpendicular to the satellite track is obtained by the geostrophy equations, which amounts to compute spatial derivatives. The geostrophic currents are computed using filtered and unfiltered 1 Hz SLA, filtered 40 Hz SLA and glider DH. The unfiltered 40 Hz signal led to unrealistic velocities, which were thus discarded from the subsequent discussions.

2.4.5. Correction to glider velocities

The depth-averaged absolute currents retrieved from the GPS glider positioning (Sec. 2.2) were used to correct the surface geostrophic current, following the method described in Bouffard et al. (2012): the difference between the relative depth-average geostrophic currents (computed from DH) and the absolute DAV (computed from glider GPS) constitutes a reliable estimation

of the absolute geostrophic current at the reference level. Hence if this velocity difference is added to the relative geostrophic current at each depth level, the absolute geostrophic current is obtained.

The condition for this correction to be valid is that the vertically averaged horizontal ageostrophic velocity is negligible with respect to the DAV. Bouffard et al. (2010) showed that barotrophic high-frequency motion, tidal or Ekman currents constitute negligible contributions. Scatterometer satellite data (not shown) confirmed the weak wind intensity in the studied area.

3. Results

3.1. Glider temperature and depth-average velocity

The glider profiles provided a high-resolution sampling of the whole water column (Fig. 2), especially in the coastal area (the last 20 km of the track) and evidenced the strong stratification characteristic of the region at that time of the year.

The estimated DAV were on the order of 2 cm s^{-1} in the southernmost part of the glider trajectory and on the order of 10 cm s^{-1} near the the end point, with a preferred north-westward orientation.

3.2. Dynamic height and absolute dynamic topography

The glider DH and the alimetry ADT at 1 Hz and 40 Hz obtained with the processing described in the previous section, are shown in Fig. 3. The first observation is the weak amplitudes (≈2 cm) and gradients present all along the track. Such values are close to the accuracy expected for the SLA measurements by SARAL/AltiKa and illustrate the low dynamic activity at that time of the year. Note that along the glider trajectory, the MDT (not shown) exhibits only weak changes, the value ranging from -1 cm at 38.2°N to 0 cm close to the island at 38.78°N. However these variations have to be taken into account, given the weak amplitude of along-track SLA.

The three filtered curves have in common the relatively sharp increase in the northern part of the track, which will result in a north-westward current (see next section). Another relevant feature is the apparent shift, roughly 5 km, between the glider DH and the 40 Hz filtered ADT. The shift is easily identifiable by observing the local minima and maxima between 38.5 and 38.7°N. A reasonable hypothesis is to attribute it to the lack of synopticity between the measurements: the glider was deployed only 7 hours after the

altimeter pass, but the end of the trajectory took place almost 3.5 days later (Sec. 2.2).

By means of the radar HF system, the time variability of the currents can be easily assessed and the hypothesis confirmed.

3.3. Time variability

It is instructive to examine specifically the temporal variability of the currents over a period ranging from the SARAL/AltiKa pass in the region of interest and the glider recovery. To this end, two HF radar velocity fields corresponding to August 2, 12:00 and August 4, 18:00, are presented (Fig. 4). On August 2, currents described a cyclonic circulation (red arrows in the figure) centred at 38.65°N, 0.9°E; the strongest currents, located south-west of Ibiza, were dominantly north-westward with a velocity on the order of 20 cm s^{-1} and a jet width of 21 km. In the southernmost part of the HF radar area, the velocity was mostly westward. On August 4, the cyclonic circulation persisted and intensified; the center slightly moved south-westward and the jet increased its width to 26 km. The circulation west of Ibiza, above 38.8°N, also changed, with the development of an anticyclonic circulation center east of Ibiza with a 10 km radius and velocities above 25 cm s^{-1}.

The cross-track velocities (black arrows) evidence the evolution of circulation, in particular the overall cyclonic circulation maintained through the G-AltiKa mission and the displacements of the circulation center. The distances between the successive locations where the velocity changes direction with respect to the altimeter track (black squares in Fig. 4) constitute a valuable information on the currents variability and allows one to address the lack of synopticity between the glider and satellite measurements. Calculation yields values on the order of 5 km between two consecutive days.

3.4. Velocity structure

The geostrophic velocities derived from the ADT (1 Hz and 40 Hz) and the DH can be compared to the HF radar velocities (Fig. 5). Both the HF radar and the 1 Hz data (top sub-figures) depict the cyclonic circulation, yet the 1 Hz data provides more details in the southernmost part of the track. The maximal velocity is larger with the 1 Hz data (32 cm s^{-1}) than with the HF radar (21 cm s^{-1}). These discrepancies are attributed to the 6 km averaging radius applied for the smoothing of the radials and to the error on the HF radar velocities. This error depends on the HF radar and current geometry, as well as on the weather conditions, and has an order of

magnitude of 10 cm s^{-1} (e.g., Chapman et al., 1997; Yoshikawa et al., 2006; Roesler et al., 2013).

The 40 Hz and the glider data (Fig. 5, bottom sub-figures) offer an increased spatial resolution of the features. The dominant westward current in the upper part of the track (north of 38.7°N) is well reproduced by both platforms, while the currents in the lower part of the track exhibit a similar pattern but clearly differ from the overall eastward velocities obtained with 1 Hz and HF radar data. The apparent disagreement between the 1 Hz and the 40 Hz data could be explained by the combination of different steps in the two processing chain DUACS and PEACHI: 1. the projection onto the theoretical track for DUACS; 2. the removal of the mean profile for DUACS. The 40 Hz data maximal velocity (34.9 cm s^{-1}), located about 5 km off Ibiza island, is comparable to the 1 Hz maximal velocity. The glider did not permit the computation of such high velocities since its trajectory was stopped before reaching the area.

The width of the coastal jet is difficult to assess from the results of Fig. 5, since the different platforms did not provide data on the same portions of the track. For example with the 40 Hz SLA, it is possible to come very close to the coast (less than 5 km). An approximate value for the coastal jet width is 30 km.

While this comparison highlights the different scales captured by the various platforms, it is still necessary to quantify the agreement between the four velocity fields, taking into account the lack of synopticity between the glider and the altimeter.

3.5. Statistical comparison

The cross-track velocity fields obtained with different platforms and resolutions are compared using two simple statistical measures: the correlations and the root mean square (RMS) of their differences. The statistics are evaluated on the section of the track covered by the HF radar, the glider and SARAL/AltiKa altimeter, i.e., between 38.405°N (the southernmost latitude reached by the HF radar) and 38.767°N (the northernmost position of the glider). The distance between these two points is 41.3 km. The number of samples over which the statistics are computed (238 points) guarantees a statistical significance close to 1.

If the shift existing between glider and altimeter measurements is not taken into account, the statistical measures will not properly capture the similarities between the fields. For this reason, both the correlations and

the RMS are computed after applying a spatial lag to the glider velocities. The impact of this lag is obvious, as illustrated here: without any lag, the RMS (correlation) between the glider and 40 Hz velocities is 15.21 cm s^{-1} (3.68%), whereas with a 5 km lag, consistent with Sec. 3.2, the RMS (correlation) decreases (increases) to 9.72 ms^{-1} (63.67%). Tests with different lags demonstrated that the value leading to the lowest RMS (and highest correlation) is 5.054 km. This value is then used for all the following calculation.

The agreement between altimetry, glider and HF radar cross-track velocities is summarized by a Taylor diagram (Taylor, 2001) (Fig. 6). The glider derived velocity is chosen as the reference for the comparison. The standard deviations (STD) of the velocity fields (represented as the radial distance from the origin) range from 7.75 cm s^{-1} for the HF radar to 15.93 cm s^{-1} for the filtered 1 Hz data. The glider and 40 Hz velocities have similar STD (11.31 cm s^{-1} and 10.88 cm s^{-1}, respectively). The correlations calculated with respect to the glider velocities (azimuthal position) spread between 0.45 (HF radar) to 0.64 (40 Hz data).

The centred RMS differences between the platforms (represented as the distances between the reference and the corresponding points) confirm that the best agreement is obtained between the glider and the 40 Hz data (9.72 cm s^{-1}). With the 40 Hz data, the filtering is essential to assure a compatibility with the other platforms measurements.

4. Conclusions

The description of mesoscale processes in the coastal area using observations constitutes a new challenge in oceanography for the present decade, and this challenge has to be tackled by a multi-platform approach. The work presented here is focused on a coastal current southwest of Ibiza, in the Balearic Sea.

The measurements from in situ (glider) and remote-sensed (HF radar, altimeter) sensors acquired between August 1 and 5, 2013, south-west of Ibiza, were processed in order to provide the velocity along the SARAL/AltiKa track. Despite the weak gradients observed in the DH and ADT signals, all the platforms coincided in the existence of a north-westward coastal current less than 20 km off Ibiza, with an intensity exceeding 20 cm s^{-1}. Further offshore, the velocity structure obtained with 1 Hz filtered altimetry data and HF radar differ from those computed using 40 Hz altimetry or glider DH data. These differences are explained by the different processing steps of

1 Hz and 40 Hz products, and by the large averaging radius used on the HF radar radials. Moreover, the weak amplitudes and gradients observed in the DH and ADT signals, on the order of the expected accuracy of the AltiKa instrument, should induce caution in the interpretation. Another element to take into consideration is the sensitivity to the selected MDT.

The filtered 40 Hz ADT and the glider DH provided a remarkably similar circulation patterns, with the same alternation of north-westward and south-eastward currents and comparable intensities along the glider trajectory. Nevertheless, a 5 km spatial shift, resulting from the different times of measurement of the platforms, appeared between the velocity structures. The 5 km estimation of the shift is consistent with the temporal variations observed with the HF radar system over the period of the mission. The statistics computed after applying a spatial lag to the glider DH yielded a correlation of 63% and a RMS difference below 10 cm s^{-1}, which is the order of magnitude of the error for the HF radar velocities.

Though the presented work is focused on the surface velocities, the complementarity of the different components of the observing system is clear: the 40 Hz SLA data from SARAL/Altika, combined with the Mediterranean Sea MDT, offer a detailed representation of the cross-track current. In particular, these data allow one to derive the geostrophic velocity less than 5 km from the coast, which was not possible in earlier altimetry mission. On the other hand, the glider has the unique capability of performing measurements profiles over the water column, with an horizontal resolution below 1 km. The HF radar system is the unique facility that combines an extended spatial coverage (more than 70 km offshore) with a temporal resolution of 1 hour. It is thus the adequate tool to address the possible synopticity issue between the altimeter and the glider. Finally, the three platforms have in common that they are highly robust systems able to monitor hydrographic conditions in the study area, even under adverse meteorological conditions.

All in all, this comparison exercise is of particular interest to validate altimetric data, especially AltiKa, in the coastal band. It also emphasizes the relevance of cross-platform approaches to study the coastal ocean dynamics and the for additional sources of validation for the currents (drifters for example) and the necessity to acquire in situ measurements closer to the coast in order to confirm the velocities deduced from high-resolution altimetry.

Acknowledgements

SARAL IGDR are produced by CNES SPA Team as part of the SSALTO ground processing segment, and distributed by AVISO, with support from CNES SALP project. G-AltiKa experiment was carried out in the frame of MyOcean2 EU FP7 funded project, with substantial support from SOCIB. Glider operations were partially funded by JERICO and PERSEUS FP7 projects. The authors would like to extend special thanks to S. Cusí, C. Castilla. J.-P. Beltrán, K. Sebastián and I. Lizarán for their efficient work during G-AltiKa experiment, and to I. Pujol and C. Pelloquin (CLS) for providing us with the near-real time data. Additional funding from the Local Government of the Balearic Islands (CAIB-51/2011 Grant) is also acknowledged. C. Troupin post-doctoral position is funded by MyOcean2 EU FP7 project. This work is a contribution to the SARAL/AltiKa science team.

References

Amores, A., Monserrat, S., Marcos, M., 2013. Vertical structure and temporal evolution of an anticyclonic eddy in the Balearic Sea (western Mediterranean). J. Geophys. Res. 118, 2097–2106. doi:10.1002/jgrc.20150. URL: http://onlinelibrary.wiley.com/doi/10.1002/jgrc.20150/abstract

Bignami, F., Böhm, E., D'Acunzo, E., D'Archino, R., Salusti, E., 2008. On the dynamics of surface cold filaments in the Mediterranean Sea. J. Mar. Syst. 74, 429–442. doi:10.1016/j.jmarsys.2008.03.002. URL: http://www.sciencedirect.com/science/article/pii/S0924796308000547

Blackman, R.B., Tukey, J.W., 1959. The Measurement of Power Spectra, From the Point of View of Communications Engineering. Dover, New York. ISBN: 978-0486605074.

Bouché, V., 2003. About process times in some deepwater formation events in the Mediterranean Sea. J. Mar. Syst. 38, 305–321. doi:10.1016/S0924-7963(02)00249-X. URL: http://www.sciencedirect.com/science/article/pii/S092479630200249X

Bouffard, J., Pascual, A., Ruiz, S., Faugère, Y., Tintoré, J., 2010. Coastal and mesoscale dynamics characterization using altimetry and gliders: A case study in the Balearic Sea. J. Geophys. Res. 115, . doi:10.1029/2009JC006087.
URL: http://www.agu.org/pubs/crossref/2010/2009JC006087.shtml

Bouffard, J., Renault, L., Ruiz, S., Pascual, A., Dufau, C., Tintoré, J., 2012. Sub-surface small-scale eddy dynamics from multi-sensor observations and modeling. Prog. Oceanogr. 106, 62–79. doi:10.1016/j.pocean.2012.06.007.
URL: http://www.sciencedirect.com/science/article/pii/S0079661112000705

Bronner, E., 2013. SARAL/AltiKa Products Handbook. Technical Report Issue 2 rev. 3. CNES. 87 pp.

Chapman, R.D., Shay, L.K., Graber, H.C., Edson, J.B., Karachintsev, A., Trump, C.L., Ross, D.B., 1997. On the accuracy of hf radar surface current measurements: Intercomparisons with ship-based sensors. J. Geophys. Res. 102, 18737–18748. doi:10.1029/97JC00049.
URL: http://onlinelibrary.wiley.com/doi/10.1029/97JC00049/abstract

Cipollini, P., Beneviste, J., Bouffard, J., Emery, W., Fenoglio-Marc, L., Gommenginger, C., Griffin, D., Hoyer, J., Kurapov, A., Madsen, K., Mercier, F., Miller, L., Pascual, A., Ravichandran, M., Shillington, F., Snaith, H., Strub, T., Vandemark, D., Vignudelli, S., Wilkin, J., Woodworth, P., Zavala-Garay, J., 2010. The role of altimetry in coastal observing systems. in: Hall, J., Harrison, D., Stammer, D. (Eds.), Proceedings of OceanObs'09: Sustained Ocean Observations and Information for Society, Vol. 2. European Space Agency. WPP-306, pp. 181–191.
URL: http://eprints.soton.ac.uk/340378/

Escudier, R., Bouffard, J., Pascual, A., Poulain, P.M., Pujol, M.I., 2013. Improvement of coastal and mesoscale observation from space: application to the Northwestern Mediterranean Sea. Geophys. Res. Lett. 40, 2148–2153. doi:10.1002/grl.50324.
URL: http://onlinelibrary.wiley.com/doi/10.1002/grl.50324/pdf

García-Lafuente, J.M., López-Jurado, J.L., Cano-Lucaya, N., Vargas-Yáñez,

M., Aguiar-Garcia, J., 1995. Circulation of water masses through the Ibiza Channel. Oceanol. Acta 18, 245–254.

Gascard, J.C., 1991. Open Ocean Convection and Deep Water Formation Revisited in the Mediterranean, Labrador, Greenland and Weddell Seas. in: Chu, P., Gascard, J.C. (Eds.), Deep Convection and Deep Water Formation in the Oceans Proceedings of the International Monterey Colloquium on Deep Convection and Deep Water Formation in the Oceans. Elsevier. volume 57 of *Elsevier Oceanography Series*, pp. 157–181. doi:10.1016/S0422-9894(08)70066-7.
URL: http://www.sciencedirect.com/science/article/pii/S0422989408700667

Harlan, J., Terrill, E., Hazard, L., Keen, C., Barrick, D., Whelan, C., Howden, S., Kohut, J., 2010. The integrated ocean observing system high-frequency radar network: Status and local, regional, and national applications. Mar. Technol. Soc. J. 44, 122–132. doi:10.4031/mtsj.44.6.6.
URL: http://www.ingentaconnect.com/content/mts/mtsj/2010/00000044/00000006/art00017

Heslop, E.E., Ruiz, S., Allen, J., López-Jurado, J.L., Renault, L., Tintoré, J., 2012. Autonomous underwater gliders monitoring variability at choke points in our ocean system: A case study in the Western Mediterranean Sea. Geophys. Res. Lett. 39, L20604. doi:10.1029/2012GL053717.
URL: http://onlinelibrary.wiley.com/doi/10.1029/2012GL053717/full

Jones, E., Oliphant, T., Peterson, P., et al., 2001. SciPy: Open source scientific tools for Python.

Juza, M., Renault, L., Ruiz, S., Tintoré, J., 2013. Origin and pathways of Winter Intermediate Water in the Northwestern Mediterranean Sea using observations and numerical simulation. J. Geophys. Res. 118, 6621–6633. doi:10.1002/2013JC009231.
URL: http://onlinelibrary.wiley.com/doi/10.1002/2013JC009231/full

La Violette, P.E., Tintoré, J., Font, J., 1990. The surface circulation of the Balearic Sea. J. Geophys. Res. 95, 1559–1568. doi:10.1029/JC095iC02p01559.

URL: http://onlinelibrary.wiley.com/doi/10.1029/JC095iC02p01559/pdf

Le Traon, P.Y., 2013. From satellite altimetry to Argo and operational oceanography: three revolutions in oceanography. Ocean Sci. 9, 901–915. doi:10.5194/os-9-901-2013.
URL: http://www.ocean-sci.net/9/901/2013/

Mason, E., Pascual, A., 2013. Multiscale variability in the Balearic Sea: An altimetric perspective. J. Geophys. Res. 118, 3007–3025. doi:10.1002/jgrc.20234.
URL: http://onlinelibrary.wiley.com/doi/10.1002/jgrc.20234/abstract

Merckelbach, L., Briggs, R.D., Smeed, D., Griffiths, G., 2008. Current measurements from autonomous underwater gliders. in: Current Measurement Technology, 2008. CMTC 2008. IEEE/OES 9th Working Conference on Measurement Technology, Inst. Electr. Eng., Piscataway. pp. 61–67. doi:10.1109/CCM.2008.4480845.

Monserrat, S., López-Jurado, J., Marcos, M., 2008. A mesoscale index to describe the regional circulation around the Balearic Islands. J. Mar. Syst. 71, 413 – 420. doi:10.1016/j.jmarsys.2006.11.012.
URL: http://www.sciencedirect.com/science/article/pii/S0924796307002011

Pascual, A., Bouffard, J., Ruiz, S., Buongiorno Nardelli, B., Vidal-Vijande, E., Escudier, R., Sayol, J.M., Orfila, A., 2013. Recent improvements in mesoscale characterization of the western Mediterranean Sea: synergy between satellite altimetry and other observational approaches. Sci. Mar. 77, 19–36. doi:10.3989/scimar.03740.15A.
URL: http://www.icm.csic.es/scimar/index.php/secId/6/IdArt/4179/

Pascual, A., Ruiz, S., Tintoré, J., 2010. Combining new and conventional sensors to study the Balearic Current. Sea Technol. 51, 32–36.
URL: http://www.sea-technology.com/features/2010/0710/balearic_current.html

Pinot, J.M., López-Jurado, J., Riera, M., 2002. The CANALES experiment (1996-1998). Interannual, seasonal, and mesoscale variability of the circulation in the Balearic Channels. Prog. Oceanogr. 55, 335–370. doi:10.1016/S0079-6611(02)00139-8.
URL: http://www.sciencedirect.com/science/article/pii/S0079661102001398

Pinot, J.M., Tintoré, J., Gomis, D., 1994. Quasi-synoptic mesoscale variability in the Balearic Sea. Deep-Sea Res. I 41, 897 – 914. doi:10.1016/0967-0637(94)90082-5.
URL: http://www.sciencedirect.com/science/article/pii/0967063794900825

Rio, M.H., Pascual, A., Poulain, P.M., Menna, M., Barceló, B., Tintoré, J., 2014. Computation of a new Mean Dynamic Topography for the Mediterranean Sea from model outputs, altimeter measurements and oceanographic in-situ data. Ocean Sci. Discuss. 11, 1–38.

Rio, M.H., Poulain, P.M., Pascual, A., Mauri, E., Larnicol, G., Santoleri, R., 2007. A Mean Dynamic Topography of the Mediterranean Sea computed from altimetric data, in-situ measurements and a general circulation model. J. Mar. Syst. 65, 484–508. doi:10.1016/j.jmarsys.2005.02.006.
URL: http://www.sciencedirect.com/science/article/pii/S0924796306003083

Roesler, C.J., Emery, W.J., Kim, S.Y., 2013. Evaluating the use of high-frequency radar coastal currents to correct satellite altimetry. J. Geophys. Res. 118, 3240–3259. doi:10.1002/jgrc.20220.
URL: http://onlinelibrary.wiley.com/doi/10.1002/jgrc.20220/full

Rubio, A., Barnier, B., Jordà, G., Espino, M., Marsaleix, P., 2009. Origin and dynamics of mesoscale eddies in the Catalan Sea (NW Mediterranean): Insight from a numerical model study. J. Geophys. Res. 114, C06009. doi:10.1029/2007JC004245.
URL: http://onlinelibrary.wiley.com/doi/10.1029/2007JC004245/full

Ruiz, S., Garau, B., Martnez-Ledesma, M., Casas, B., Pascual, A., Vizoso, G., Bouffard, J., Heslop, E., Alvarez, A., Testor, P., Tintoré, J., 2012.

New technologies for marine research: five years of glider activities at IMEDEA. Sci. Mar. 76, 261270. doi:10.3989/scimar.03622.19l.
URL: http://scientiamarina.revistas.csic.es/index.php/scientiamarina/article/view/1372/1471

Ruiz, S., Pascual, A., Garau, B., Faugère, Y., Alvarez, A., Tintoré, J., 2009a. Mesoscale dynamics of the Balearic Front, integrating glider, ship and satellite data. J. Mar. Syst. 78 (supplement), S3–S16. doi:10.1016/j.jmarsys.2009.01.007.
URL: http://www.sciencedirect.com/science/article/pii/S0924796309001365

Ruiz, S., Pascual, A., Garau, B., Pujol, I., Tintoré, J., 2009b. Vertical motion in the upper ocean from glider and altimetry data. Geophys. Res. Lett. 36, L14607. doi:10.1029/2009GL038569.
URL: http://www.agu.org/pubs/crossref/2009/2009GL038569.shtml

Salusti, E., 1998. Satellite images of upwellings and cold filament dynamics as transient effects of violent air-sea interactions downstream from the island of Sardinia (western Mediterranean Sea). J. Geophys. Res. 103, 3013–3031. doi:10.1029/97JC01914.
URL: http://onlinelibrary.wiley.com/doi/10.1029/97JC01914/abstract

Send, U., Font, J., Krahmann, G., Millot, C., Rhein, M., Tintoré, J., 1999. Recent advances in observing the physical oceanography of the western Mediterranean Sea. Prog. Oceanogr. 44, 37–64. doi:10.1016/S0079-6611(99)00020-8.
URL: http://www.sciencedirect.com/science/article/pii/S0079661199000208

Smith, S., 2002. Digital Signal Processing: A Practical Guide for Engineers and Scientists. California Technical Publishing. 1st edition. ISBN: 978-0750674447.
URL: http://www.dspguide.com/

Taveneau, N., Robert, F., Richard, J., Steunou, N., Sengenes, P., 2011. Characteristics and performances of the AltiKa radiometer of SARAL mission. in: Geoscience and Remote Sensing Symposium (IGARSS), 2011 IEEE International, pp. 3979–3982. doi:10.1109/IGARSS.2011.6050103.

Taylor, K.E., 2001. Summarizing multiple aspects of model performance in a single diagram. J. Geophys. Res. 106, 7183–7192. doi:10.1029/2000JD900719.
URL: http://onlinelibrary.wiley.com/doi/10.1029/2000JD900719/abstract

Testor, P., Meyers, G., Pattiaratchi, C., Bachmayer, R., Hayes, D., Pouliquen, S., de la Villeon, L.P., Carval, T., Ganachaud, A., Gourdeau, L., Mortier, L., Claustre, H., Taillandier, V., Lherminier, P., Terre, T., Visbeck, M., Karstensen, J., Krahman, G., Alvarez, A., Rixen, M., Poulain, P.M., Osterhus, S., Tintore, J., Ruiz, S., Garau, B., Smeed, D., Griffiths, G., Merckelbach, L., Sherwin, T., Schmid, C., Barth, J.A., Schofield, O., Glenn, S., Kohut, J., Perry, M.J., Eriksen, C., Send, U., Davis, R., Rudnick, D., Sherman, J., Jones, C., Webb, D., Lee, C., Owens, B., 2010. Gliders as a Component of Future Observing Systems. in: Hall, J., Harrison, D., Stammer, D. (Eds.), Proceedings of OceanObs'09: Sustained Ocean Observations and Information for Society, Vol. 2. European Space Agency. doi:10.5270/oceanobs09.cwp.89.
URL: http://www.oceanobs09.net/proceedings/cwp/cwp89/index.php

Tintoré, J., Vizoso, G., Casas, B., Heslop, E., Pascual, A., Orfila, A., Ruiz, S., Martínez-Ledesma, M., Torner, M., Cusí, S., Diedrich, A., Balaguer, P., Gómez-Pujol, L., Álvarez Ellacuria, A., Gómara, S., Sebastian, K., Lora, S., Beltrán, J.P., Renault, L., Juzà, M., Álvarez, D., March, D., Garau, B., Castilla, C., Cañellas, T., Roque, D., Lizarán, I., Pitarch, S., Carrasco, M.A., Lana, A., Mason, E., Escudier, R., Conti, D., Sayol, J.M., Barceló, B., Alemany, F., Reglero, P., Massuti, E., Vélez-Belchí, P., Ruiz, J., Oguz, T., Gómez, M., Álvarez, E., Ansorena, L., Manriquez, M., 2013. SOCIB: The Balearic Islands Coastal Ocean Observing and Forecasting System Responding to Science, Technology and Society Needs. Mar. Technol. Soc. J. 47, 101–117. doi:10.4031/MTSJ.47.1.10.
URL: http://www.ingentaconnect.com/content/mts/mtsj/2013/00000047/00000001/art00010

Tintoré, J., Wang, D.P., La Violette, P.E., 1990. Eddies and thermohaline intrusions of the shelf/slope front off the northeast Spanish coast. J. Geophys. Res. 95, 1627–1633. doi:10.1029/JC095iC02p01627.

URL: http://onlinelibrary.wiley.com/doi/10.1029/JC095iC02p01627/pdf

Verron, J., 2013. SARAL/AltiKa: A Ka Band Altimetric Mission. Aviso Users Newsletter 10, 1–15.
URL: http://www.aviso.altimetry.fr/uploads/media/aviso_special_issue_Saral_news10_01.pdf

Vignudelli, S., Kostianoy, A., Cipollini, P., Benveniste, J. (Eds.), 2011. Coastal Altimetry. Springer. doi:10.1007/978-3-642-12796-0. ISBN: 978-3-642-12795-3.
URL: http://link.springer.com/book/10.1007/978-3-642-12796-0/page/1

Wang, D.P., Vieira, M.E.C., Salat, J., Tintor, J., La Violette, P.E., 1988. A shelf/slope frontal filament off the northeast spanish coast. J. Mar. Res. 46, 321–332. doi:10.1357/002224088785113586.
URL: http://www.ingentaconnect.com/content/jmr/jmr/1988/00000046/00000002/art00005

Yoshikawa, Y., Masuda, A., Marubayashi, K., Ishibashi, M., Okuno, A., 2006. On the accuracy of HF radar measurement in the Tsushima Strait. J. Geophys. Res. 111, C04009. doi:10.1029/2005JC003232.
URL: http://onlinelibrary.wiley.com/doi/10.1029/2005JC003232/abstract

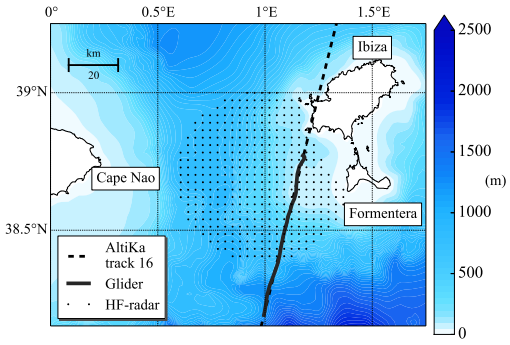

Figure 1: HF Radar, glider and altimetry data locations overlaid on the Ibiza Channel bathymetry.

Figure 2: Temperature measurements along the glider track (left) and depth-averaged velocities.

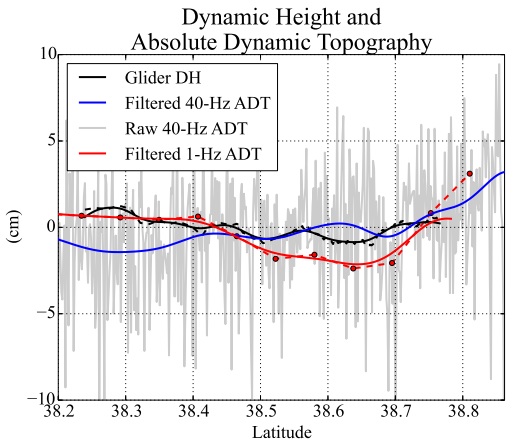

Figure 3: Absolute dynamic topography and dynamic height along SARAL track no. 16 southwest of Ibiza islands. Dashed lines represent the unfiltered glider DH and 1 Hz ADT signals.

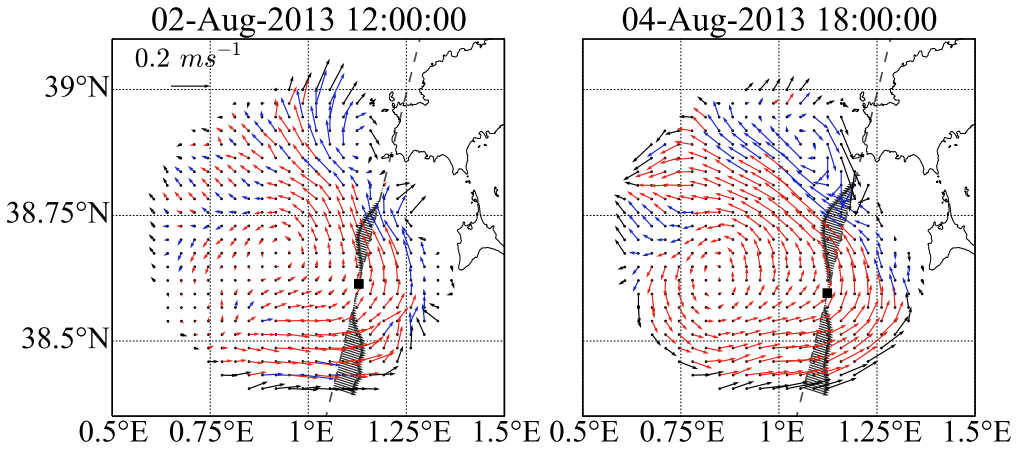

Figure 4: HF Radar velocities on August 2, 12:00 and August 4, 18:00. Red (blue) indicates positive (negative) vorticity. Black arrows represent the velocity component perpendicular to SARAL/AltiKa track (dashed line). Black squares indicate the location where the velocity changes its direction with respect to the satellite track.

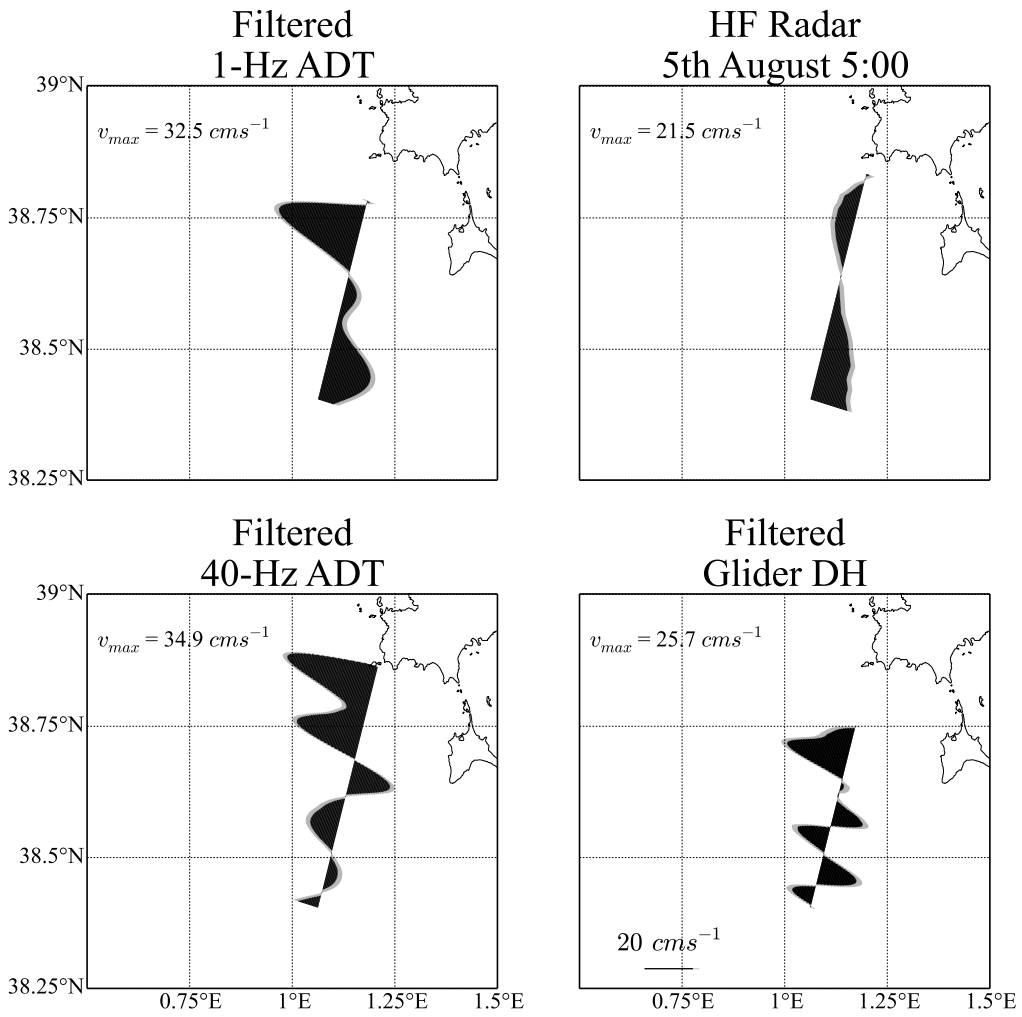

Figure 5: Cross-track velocities obtained by HF radar and by geostrophy for filtered 1 Hz, 40 Hz and glider data.

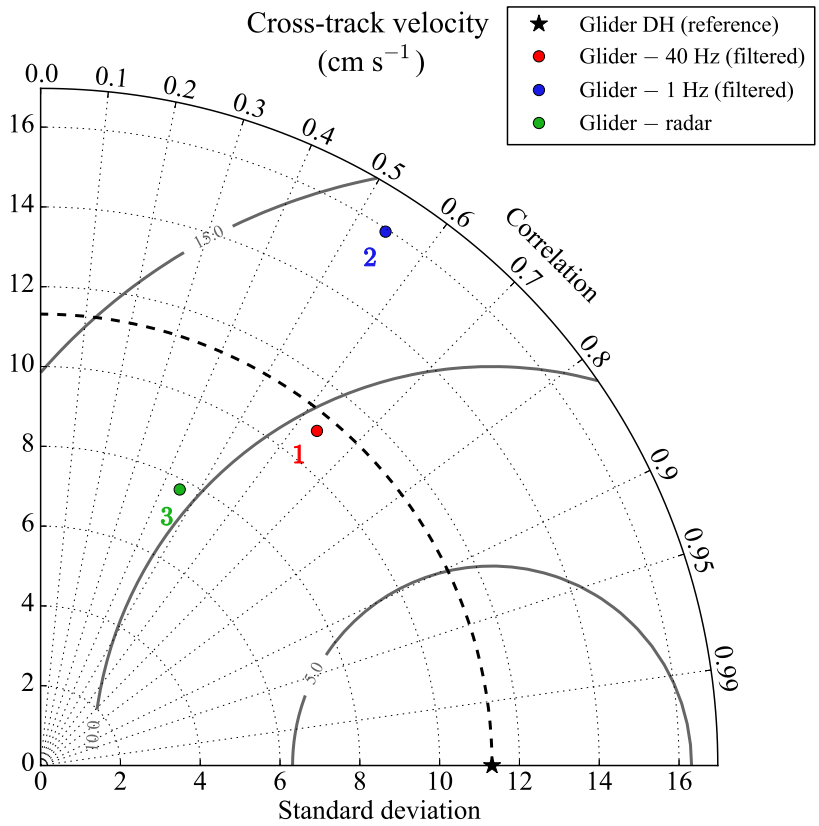

Figure 6: Taylor diagram for cross-track velocities obtained with the different platforms.